materials

MDPI

Article

In Situ Dry Chemical Synthesis of Nitrogen-Doped Activated Carbon from Bamboo Charcoal for Carbon Dioxide Adsorption

Weijun Ying [1,2], Shuo Tian [1], Huan Liu [1], Zenan Zhou [1], Grantson Kapeso [1], Jinhuan Zhong [1,*] and Wenbiao Zhang [1,*]

[1] National Engineering and Technology Research Center of Wood-Based Resources Comprehensive Utilization, Zhejiang Agriculture and Forestry University, Hangzhou 311300, China; wjying@zafu.edu.cn (W.Y.); ts0048@stu.zafu.edu.cn (S.T.); inspirelh@stu.zafu.edu.cn (H.L.); zhouzenan@stu.zafu.edu.cn (Z.Z.); grantksps@gmail.com (G.K.)

[2] Jiyang College, Zhejiang Agriculture and Forestry University, Shaoxing 311800, China

* Correspondence: goldring@live.com (J.Z.); zwb@zafu.edu.cn (W.Z.)

Abstract: In this work, nitrogen-doped bamboo-based activated carbon (NBAC) was in situ synthesized from simply blending bamboo charcoal (BC) with sodamide (SA, $NaNH_2$) powders and heating with a protection of nitrogen flow at a medium temperature. The elemental analysis and X-ray photoelectron spectra of as-synthesized NBAC showed quite a high nitrogen level of the simultaneously activated and doped samples; an abundant pore structure had also been determined from the NBACs which has a narrow size distribution of micropores (<2 nm) and favorable specific surface area that presented superb adsorption performance. The fcarbon dioxide (CO_2) adsorption of the NBACs was measured at 0 °C and 25 °C at a pressure of 1 bar, whose capture capacities reached 3.68–4.95 mmol/g and 2.49–3.52 mmol/g, respectively, and the maximum adsorption could be observed for NBACs fabricated with an SA/BC ratio of 3:1 and activated at 500 °C. Further, adsorption selectivity of CO_2 over N_2 was deduced with the ideal adsorbed solution theory ((IAST), the selectivity was finally calculated which ranged from 15 to 17 for the NBACs fabricated at 500 °C). The initial isosteric heat of adsorption (Qst) of NBACs was also determined at 30–40 kJ/mol, which suggested that CO_2 adsorption was a physical process. The results of ten-cycle adsorption-desorption experimentally confirmed the regenerated NBACs of a steady CO_2 adsorption performance, that is, the as-synthesized versatile NBAC with superb reproducibility makes it a perspective candidate in CO_2 capture and separation application.

Keywords: bamboo charcoal; bamboo-based activated carbon; N-doping activation; CO_2 adsorption; capture capacity

check for updates

Citation: Ying, W.; Tian, S.; Liu, H.; Zhou, Z.; Kapeso, G.; Zhong, J.; Zhang, W. In Situ Dry Chemical Synthesis of Nitrogen-Doped Activated Carbon from Bamboo Charcoal for Carbon Dioxide Adsorption. *Materials* **2022**, *15*, 763. https://doi.org/10.3390/ma15030763

Academic Editors: John Vakros, Evroula Hapeshi, Catia Cannilla and Giuseppe Bonura

Received: 22 December 2021
Accepted: 17 January 2022
Published: 20 January 2022

Publisher's Note: MDPI stays neutral with regard to jurisdictional claims in published maps and institutional affiliations.

Copyright: © 2022 by the authors. Licensee MDPI, Basel, Switzerland. This article is an open access article distributed under the terms and conditions of the Creative Commons Attribution (CC BY) license (https://creativecommons.org/licenses/by/4.0/).

1. Introduction

Carbon dioxide (CO_2) emission is extensively known as the reason for climate change and global warming [1]; international protocols and countermeasures have declared to achieve carbon neutrality [2]. Vast work among the academic community has been taken to alleviate the negative effect of the rapid growth of atmospheric CO_2 concentration at a global level, such as developing renewable and clean energies [3–5] and functional porous materials [6,7], and decades of research and projects on carbon capture, utilization and sequestration (CCUS) [8–10] have been conducted to reduce the influence of carbon emission. And various solid absorbents, such like activated carbon (AC) [11–14], molecular sieve [15,16], metal oxides [17] and MOF [18], Among these products, ACs have been widely applied in carbon dioxide capture due to their special pore structure, specific surface area and chemical stability, and simple processing; tremendous research efforts have focused on the adsorption capacity, selectivity and renew-ability of activated carbon products [19–24].

Activated carbon can be synthesized from multiple bioresources by chemical activation. Idrees et al. [25] reported that peanut shell-deprived AC by KOH activation featured

micropores (<1 nm) and the results showed that the structure had a positive relationship with CO_2 adsorption. Modifications can further improve the adsorbing performance. For example, various reports [7,26–28] have demonstrated that sodamide activation was a useful approach to synthesize functionalized porous carbon materials for CO_2 capture, and the nitrogen-doping method has been reported to be a versatile route for enhancing CO_2 adsorption. For example, nitrogen functionalized biochar has been applied as a renewable adsorbent for efficient CO_2 removal whose adsorption could reach up to 4.58 mmol/g and it was also found that the adsorption mainly rested with a micropore smaller than 0.80 nm [29]. N-doped AC prepared by urea and KOH co-activation using sugarcane waste [30] demonstrated a doubled CO_2 capture capacity (4.8 mmol/g) as compared with an untreated control trial sample. Other materials, such as chitosan [31], glucose [32], and their derivatives are also employed as nitrogen sources for doping AC to obtain improved CO_2 adsorption. It is essential to develop a cost-effective, commercially available raw material and an activation approach to prepare AC with high efficiency performance for a specific purpose.

Fast-growing bamboo is extensively cultivated across tropical and temperate regions which makes its value-added production sustainable around the world. Bamboo charcoal (BC) is the solid product of the pyrolysis of bamboo materials in the absence of oxygen. It is commercially available at any time in the market. The gaseous and liquid adsorption performance of bamboo charcoal and bamboo activated carbon (BAC) have been widely studied because the emerging BC/BAC has shown great potential in environmental purification. Specially designed, synthesized, and modified BC or BAC are applied in air quality improvement to remove formaldehyde [33], volatile organic compounds [34], carbon dioxide [35], sulfur dioxide, and nitrogen oxides [36], or in eradication of contaminants such as heavy metals in water [37] and antibiotics [38,39] in the pharmaceutical industry, and the wastes and leftovers of N-/P-modified bamboo charcoals are valid for soil amelioration [40] and carbon sequestration. Modified bamboo-based activated carbons prepared from bamboo and its processing residue are also used as CO_2 absorbents [41,42] for their favorable adsorption performance.

However, either phosphoric acid or alkali activation to prepare activated carbon can be harmful to the environment or cause corrosion to equipment [43]; therefore, identifying activation materials of low pollution and corrosion is important to improve conventional processes. Traditional modifications generally require tedious processing and skilled work with high costs; therefore, developing a convenient synthesis of doped AC is beneficial to both industrial and academic research. In this work, a new method is presented to prepare N-doped BAC (NBAC) by a facile one-step in situ dry chemical process by simply blending bamboo charcoal with sodamide ($NaNH_2$) in a tubular furnace activated at medium temperature (400–600 °C), which is much lower than that of conventional chemical activation that generally goes to 800 °C or beyond. The study results also showed that N-doped BACs had potential applications in CO_2 capture and separation.

2. Results and Discussion

2.1. BET Characterization

N_2 adsorption–desorption isotherm of NBAC was determined (Figure 1), which showed the adsorption performance of NBAC synthesized under controlled activation temperatures and $NaNH_2$ (SA)/BC ratios. The achieved I type isotherm indicated that the as-synthesized samples had an abundant micropore (<1 nm) structure. When SA/BC were blended at a ratio of 3:1, it can be seen that, as the activation temperature increased from 400 °C to 600 °C, the isotherm results gradually increased, proving the corresponding increment of total pore volume and N_2 adsorption capacity. When activated at 500 °C, the isotherm of NBAC almost reached a plateau at a relative pressure of 0.05, although no apparent hysteresis phenomenon appeared in that the dominated micropores were distributed in the range from 0.4–0.9 to 1.0–3.0 nm, as shown in Figure 1c; the results also implied that other NBACs obtained from different blend ratios had pores with a narrow

pore size distribution. Notably, when activated at 600 °C, both the pore volume and size distribution were relatively small, nonetheless it is slightly broader than its counterparts obtained at 400 °C or 500 °C, respectively, which may have accounted for the visually distinguishable hysteresis phenomenon that occurred to NBAC-600s, as shown in Figure 1a.

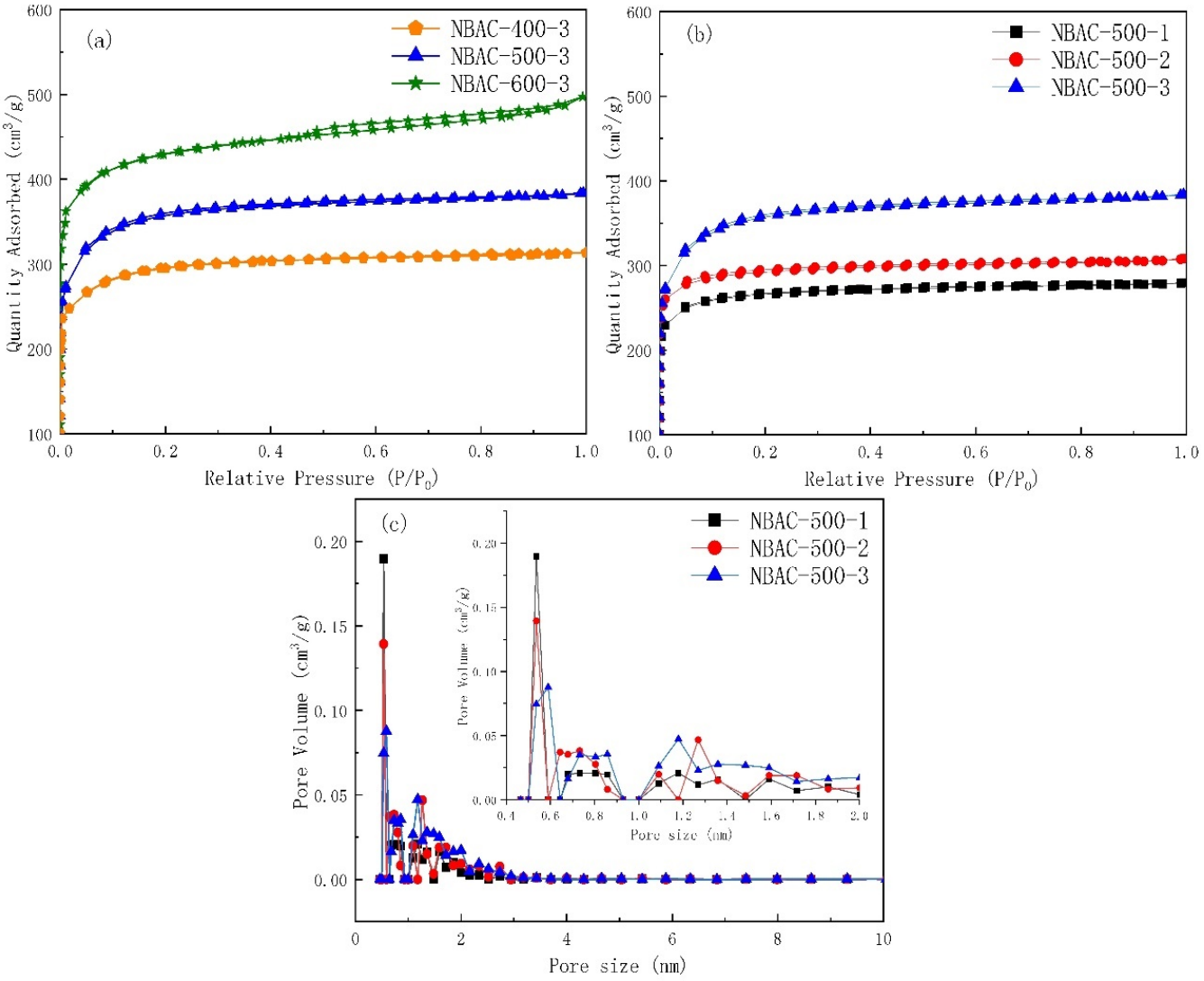

Figure 1. N_2 adsorption–desorption isotherm (**a**,**b**) of N-doped bamboo-based activated carbon synthesized by sodamide activation and its pore size distribution (**c**).

When activated at 500 °C, the BACs obtained from a low SA dosage presented that the isotherm gradually augmented with an increase in the SA/BC ratio, as seen in Figure 1b. The isotherm reached saturated adsorption at a fairly low relative pressure. When an increased dosage of SA was used in activation, a sharp enhancement in the isotherm performance occurred, most notably in the range of low relative pressure, however, it disclosed a leveling off beyond a relative pressure (P/P_0) of 0.2, which was also confirmed by the wide pore size distribution of micropores, as seen Figure 1c. Therefore, we concluded that a high SA dosage in activation may not be conducive to micropore-structured NBAC synthesis because the fierce activation could jeopardize micropore forming, causing neighboring micropores to breakdown or collapse into larger pores, and as a result, the synthesized NBAC would be less active in adsorbing small molecules such as CO_2.

The results of specific surface area (S_{BET}), total pore volume (V_{tot}), micropore volume (V_{mic}), and narrowly-distributed (0.33–1.0 nm) micropore volume ($V_{0.33–1}$) are listed in

Table 1. NBACs obtained from a low dosage of SA at 500 °C and below could be beneficial to CO_2 adsorption, although the micropore volume of NBACs obtained from a high dosage of SA tended to decline at 600 °C, owing to the excessive temperature and activation overdose that accelerated pore reaming. In fact, it jeopardized new pore structure formation, thus a negative growth for micropores that ultimately unveiled in measurement results.

Table 1. Pore parameters of NBACs synthesized from N-doping activation.

Absorbent	S_{BET} (m^2/g)	V_{tot} (cm^3/g)	V_{mic} (cm^3/g)	V_{mic}/V_{tot} (%)	$V_{(0.33–1\ nm)}$ (cm^3/g)
NBAC-400-1	756	0.300	0.271	90.33%	0.219
NBAC-400-2	927	0.370	0.322	87.03%	0.229
NBAC-400-3	1068	0.450	0.381	84.67%	0.241
NBAC-500-1	1025	0.420	0.369	87.86%	0.271
NBAC-500-2	1175	0.506	0.426	84.19%	0.285
NBAC-500-3	1286	0.631	0.508	80.51%	0.282
NBAC-600-1	1227	0.543	0.441	81.22%	0.276
NBAC-600-2	1458	0.675	0.500	74.07%	0.281
NBAC-600-3	1489	0.682	0.480	70.38%	0.233

2.2. Morphological Analysis

The microstructure patterns of NBACs were observed using a scanning electron microscope and are shown in Figure 2. Original porous bamboo morphologies were observed from the charcoal, under same low magnification (Figure 2b,c); there was no obvious surface difference between BC and BAC. Further enlargement completely exposed that the smooth surface of BAC was suffused with massive trenches and holes. The chemical etching by sodamide was effective and efficient in porosity generation. Especially, the occurrence of deep activation was observed through the hole structure that originated from the pits distributed on the vessel of bamboo, and provided a fair approach to augment surface area, therefore, making adsorption technically feasible.

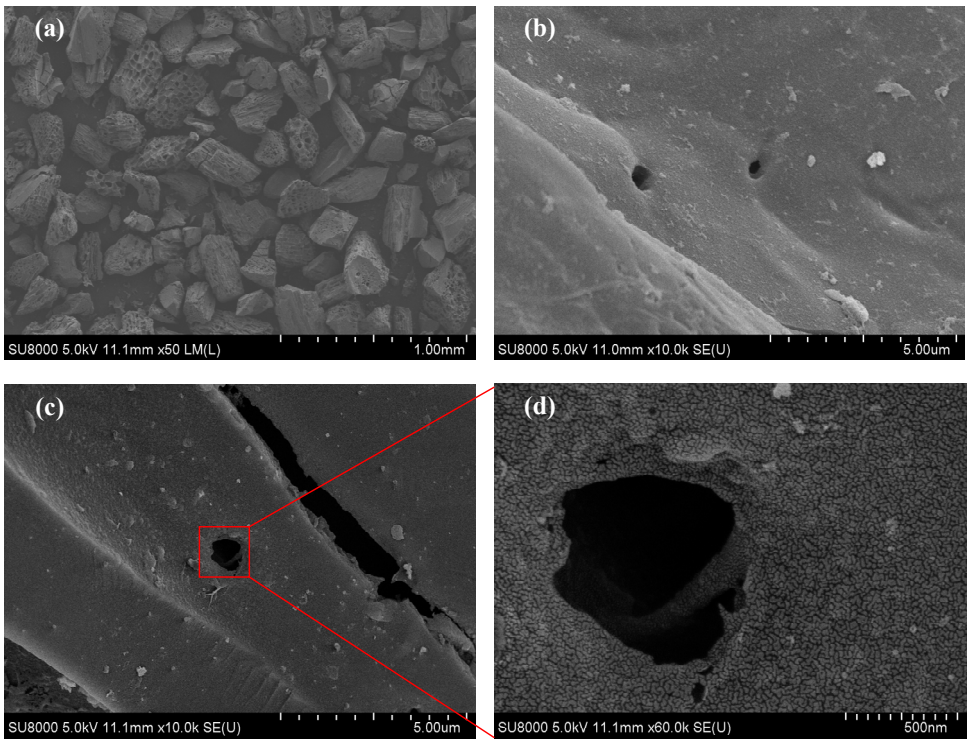

Figure 2. SEM patterns of bamboo charcoal (**a**,**b**) and N-doped bamboo-based activated carbon (**c**,**d**).

2.3. Elemental Analysis

An elemental analysis was employed to explore the composition change before and after the dry chemical processing. As shown in Table 2, the nitrogen (N) content of untreated BC is approximately 0.26%, meanwhile, the activated/doped samples average N content is 10 times more than that of the untreated BC. Simply put, an increase in the nitrogen content of BAC signaled the successful modification of samples.

Table 2. Elemental content of NBACs synthesized by N-doping activation.

Absorbent	N (wt%)	C (wt%)	H (wt%)
BC	0.26	83.5	3.12
NBAC-400-1	3.25	71.2	2.98
NBAC-400-2	3.89	72.6	3.05
NBAC-400-3	4.12	72.9	2.79
NBAC-500-1	2.51	73.2	2.43
NBAC-500-2	2.85	75.1	2.34
NBAC-500-3	3.21	74.6	2.05
NBAC-600-1	1.98	76.2	1.78
NBAC-600-2	2.15	77.3	1.81
NBAC-600-3	2.35	78.5	1.69

2.4. XPS Analysis

The XPS spectra of BC and NBAC, as shown in Figure 3a, exhibited characteristic peaks (binding energy) at 285, 399, and 532 eV, attributed to C1s, N1s, and O1s, respectively; nevertheless, a comparative strong intensity of N1s peak of NBAC-500-3 stood out.

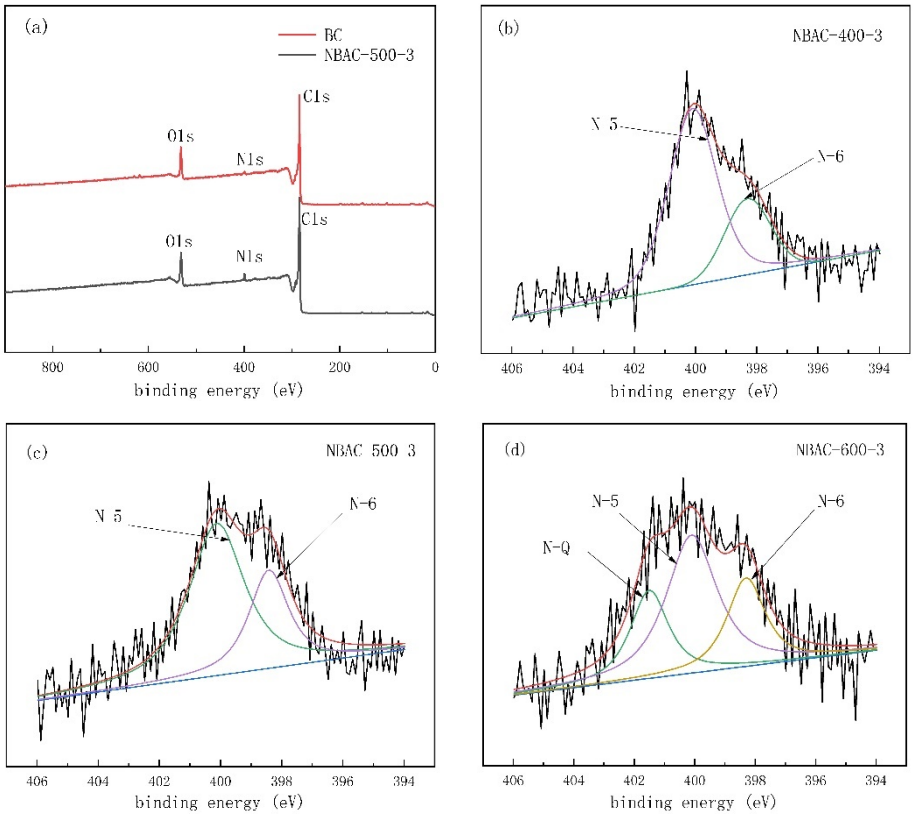

Figure 3. XPS spectra of NBAC-500-3 (**a**) and fitting curves of NBAC-400-3 (**b**), NBAC-500-3 (**c**) and NBAC-600-3 (**d**) synthesized from dry chemical activation.

Accordingly, peak-differentiating and imitating of the raw XPS spectra of nitrogen atoms was successfully analyzed. The peaks at 398.3 and 400.1 eV can be assigned to

the binding energy of pyrrolic N (N-5) and pyridinic N (N-6), respectively, as shown in Figure 3b–d. As shown in Figure 3d, an additional quaternary N (N-Q) at 401.5 eV emerged when samples were synthesized at 600 °C, supporting that the partial N-5 and N-6 phases were transforming toward the more thermodynamically stable N-Q phase, which coincided with that reported by [30]. Notably, N-5 had a favorable interaction with CO_2 molecules [44] and, based on the XPS data, doping activation at 500 °C or below can better induce functional groups that facilitate CO_2 capture. Thus, NBAC synthesized at 500 °C was, hereinafter, chosen as the object of study to explore the CO_2 capture performance.

2.5. CO_2 Adsorption Analysis

The isotherm adsorption of CO_2 and N_2 of NBACs are shown in Figure 4a,b, respectively. It can be seen that, one the one hand, the adsorption capacity was prone to decline as the temperature increased, which was a remarkable feature of a physical adsorption. On the other hand, the capacity rose constantly, even when the pressure went beyond 1 bar, which demonstrated that the BAC would continue to adsorb CO_2 or N_2 at a higher pressure. In addition, the CO_2 adsorption capacity was far higher than that of N_2, based on the collected data. For that matter, the NBAC samples also outperformed the CO_2 adsorption of three typical commercial BACs whose capacity varied from 1.43 mmol/g to 2.21 mmol/g, according to the authors' laboratory measurements at an ambient temperature (25 °C), as indicated in Table 3.

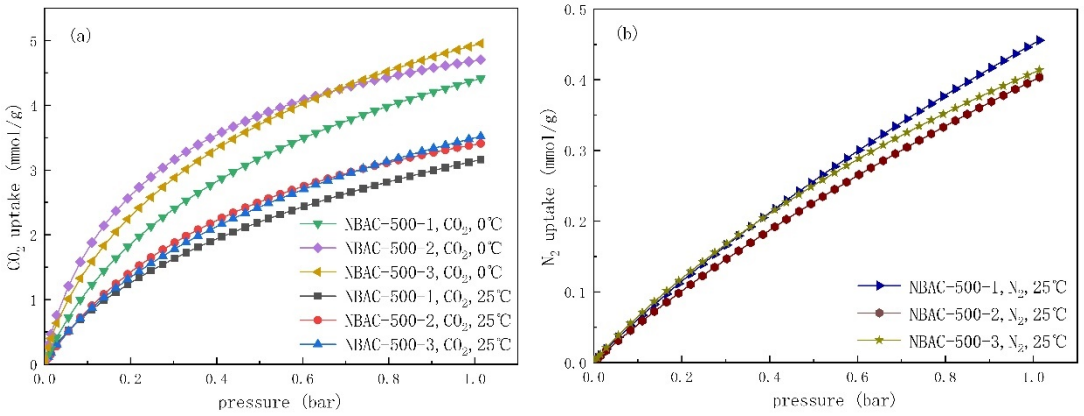

Figure 4. Adsorption isotherms of CO_2 (**a**) and N_2 (**b**) for NBACs synthesized at 500 °C.

Table 3. CO_2 and N_2 adsorption capacity for NBACs at 1 bar, at 0 °C and 25 °C.

Absorbent	CO_2 Uptake (mmol/g)		N_2 Uptake (mmol/g)
	0 °C	25 °C	25 °C
NBAC-400-1	3.68	2.49	0.33
NBAC-400-2	3.78	2.68	0.35
NBAC-400-3	3.85	2.91	0.36
NBAC-500-1	4.41	3.16	0.45
NBAC-500-2	4.71	3.41	0.40
NBAC-500-3	4.95	3.52	0.41
NBAC-600-1	4.48	3.05	0.49
NBAC-600-2	4.31	3.21	0.45
NBAC-600-3	3.76	2.78	0.46
Commercial BAC#1	/	1.43	/
Commercial BAC#2	/	1.87	/
Commercial BAC#3	/	2.21	/

The CO_2 and N_2 uptakes of BAC with pressure at 1 bar and temperature at 0 °C and 25 °C, respectively, are shown in Table 3. The uptake ranged from 3.68 to 4.95 mmol/g at 0 °C, and from 2.49 to 3.52 mmol/g at 25 °C, among which the maximum uptake occurred

for the sample obtained with high SA activent dosage (BAC-500-3). The N_2 uptake of all samples ranged from 0.33 to 0.49 mmol/g at 25 °C, which was much lower than that of CO_2 uptake with the same conditions. It also found that with more dosage of activent at 500 °C or below the CO_2 uptake of corresponding BAC were improved. It decreased as activent dosage went higher when activated at 600 °C.

It has been reported that CO_2 uptake of N-doped porous carbon can be simultaneously influenced by a narrow pore size distribution of micropores and N content [45]. In this work, it was also found that it had an above-average level upon further investigation of the data in Tables 1–3. The maximum CO_2 uptake reached 4.95 mmol/g and 3.52 mmol/g at 1 bar, at 0 °C and 25 °C, respectively, and NBAC-500-2 presented maximum narrow size distributed pores.

2.6. Analysis for Selectivity of CO_2 over N_2

The NBAC-500 samples were selected to explore their adsorption selectivity for CO_2 capture in order to assess the dynamic adsorption behavior of mixture gas containing 15 vol.% CO_2 and 85 vol.% N_2, which is a representative proportion of flue gas. The isotherm was obtained by the Langmuir–Freundlich equation (Equation (1)) from the isotherm value of CO_2 and N_2 at 1 bar and 25 °C, and adsorption selectivity could be finally deduced in accordance with the ideal adsorbed solution theory (IAST, Equation (3)). The coefficient R^2 values achieved 0.99 which showed good fitting; all detailed data and selectivity are summarized in Table 4. The selectivity of CO_2 over N_2 for NBACs was calculated to be between 15 and 17 at 25 °C, respectively. It seemed that the N content of NBAC (see Table 2) had a slightly positive effect on adsorption selectivity, which might be optimized in future works.

Table 4. Fitting results and adsorption selectivity for NBACs synthesized at 500 °C.

Absorbent	Adsorbate	q_m	b	n	R^2	Selectivity
NBAC-500-1	CO_2 N_2	8.02 2.51	0.65 0.219	0.772 0.943	0.99 0.99	15.03
NBAC-500-2	CO_2 N_2	7.47 2.23	0.84 0.218	0.865 0.946	0.99 0.99	16.87
NBAC-500-3	CO_2 N_2	7.76 1.35	0.83 0.436	0.85 0.936	0.99 0.99	16.97

The selectivity of NBAC is shown in Figure 5. It showed that optimal performance could be reached at a low pressure in that there were adequate adsorptive spots for CO_2 capture, whereas higher pressure made the N-doped BAC relatively less selective to separate CO_2.

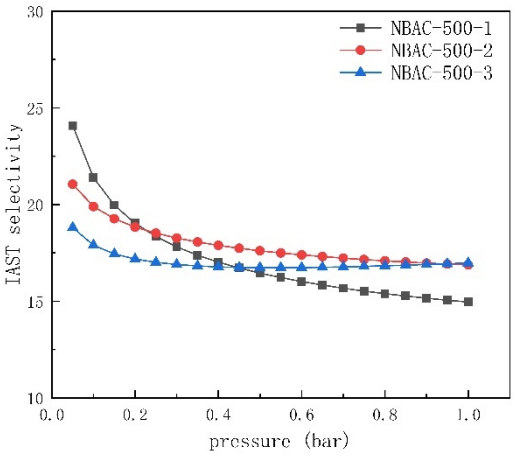

Figure 5. Adsorption selectivity of CO_2 over N_2 for NBAC synthesized at 500 °C.

2.7. Analysis for Isosteric Heat of Adsorption

An analysis of isosteric heat of adsorption is important to evaluate the adsorption performance of an absorbent; it provides the interaction information between absorbent and adsorptive. In this paper, the isosteric heat of adsorption (Qst) at 0 °C and 25 °C was determined in accordance with the Clausius–Clapeyron equation (Equation (2)). The values are illustrated in Figure 6. Should The initial CO_2 adsorption approach "0" when epitaxy method applied to the current isotherm, the initial Qst shall be 30–40 KJ/mol, a typical value of physical adsorption that proved superior adsorptive performance of NBACs in this work. A low Qst causes the NBACs to have less energy consumption during the process of desorption, that is, it is more kinetically feasible to regenerate NBACs, which helps to reduce recycling costs. As the CO_2 capture continued, the Qst had a tendency to decrease and stabilize, which may have been due to the topological non-uniformity and adsorption saturation of the NBAC samples.

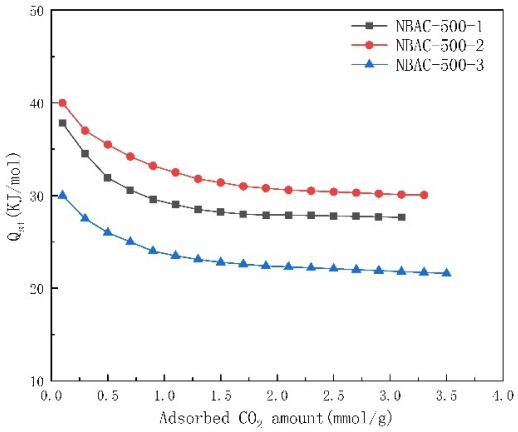

Figure 6. Isosteric heat of adsorption for NBACs synthesized at 500 °C.

2.8. Analysis for Reproducibility of CO_2 Adsorption

An analysis of reproducibility and steadiness of CO_2 adsorption is essential for practical use of activated carbons. Five experimental cycles of adsorption/desorption were conducted to consider the usability at 1 bar and 25 °C. The results for those regenerated NBACs are shown in Figure 7. Approximately 93% of the adsorption capacity (3.27 mmol/g for the tenth cycle measurement as compared with 3.52 mmol/g for the virgin NBAC-500-3) was retained even after the 10-cycle measurement which aligned with the Qst results, suggesting that the dry chemically synthesized NBACs could be a perspective candidate for industrial use in CO_2 adsorption and separation.

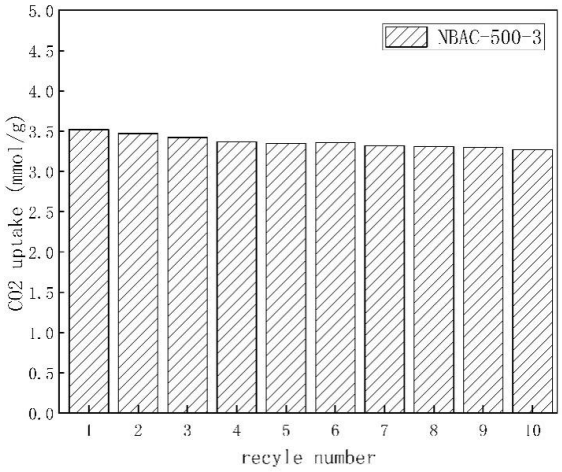

Figure 7. Adsorption/desorption experimental results for NBAC synthesized at 500 °C.

3. Experimental Section

3.1. Materials

Powder bamboo charcoal (40–60 mesh) was purchased from Zhejiang Wanlin Biotech Co, Ltd., Hangzhou, China, with pyrolysis at 750 °C for 7 days, the charcoal was oven-dried at 105 °C prior to use. Sodamide (SA, $NaNH_2$) and hydrochloric acid (37%, HCl) were purchased from Shanghai Aladdin Biochemical Technology Co., Ltd., Shanghai, China. The reagents were used as received.

3.2. Synthesis of N-Doped Bamboo-Based Activated Carbon (NBAC)

The blended SA/BC samples (the blend ratio was set at 1:1, 2:1, and 3:1, respectively) were placed under an N_2 atmosphere by applying a tube furnace (LTKC-8-16, Hangzhou Lantian Instrument Co., Ltd., Hangzhou, China), and the temperature was set at 400, 500, and 600 °C, for 2 h, respectively. Then, the raw N-doped bamboo-based activated carbon (NBAC) powders were obtained after cooling down to an ambient temperature. The NBAC samples were further rinsed using diluted hydrochloric acid (10%) to neutralize the residue and resultant of the activation and remove possible ash in the bamboo charcoal samples. The samples were termed as NBAC-x-y, where x refers to the activation temperature and y the blend ratio of $NaNH_2$/BC.

3.3. Characterization

The surface morphologies of the samples were observed by field emission scanning electron microscopy (SEM, Hitachi SU 8010, Tokyo, Japan) at the emission voltage of 5 KV. The synthesized samples were sprayed with gold prior to observation. The elements (C, H and N) were measured by elemental analyzer (EA, Vario EL cube, Germany Elementary, Hesse, Germany) applying CHN mode. The specific surface area (SSA), as well as pore volume and pore size distribution were determined by an automated adsorption system (ASAP 2020, Micromeritics, Norcross, GA, USA) using the Brunauer–Emmett–Teller (BET) equations with nitrogen gas physisorption at 77 K. The surface elemental compositions were analyzed by X-ray photoelectron spectroscopy (XPS, Thermo Scientific K-Alpha, Waltham, MA, USA) with primary photon energies of 1486.6 eV.

3.4. CO_2 Adsorption Measurement and Calculation

All NBAC samples were vacuum degassed at 300 °C for 6 h prior to adsorption measurement, followed by CO_2 adsorption isotherm measurements at a pressure of 1.0 bar and temperatures of 0 °C and 25 °C. To evaluate the gas adsorption selectivity, the N_2 adsorption isotherm of samples was also measured at 25 °C and pressure at 1 bar.

Adsorption heat and adsorption selectivity was calculated by the single site Langmuir–Freundlich equation (Equation (1)):

$$q = \frac{q_m b p^n}{1 + b p^n} \tag{1}$$

where p refers to the balancing pressure of gas expressed in MPa, q is the unit adsorption capacity of NBAC expressed in mmol, q_m is the saturated adsorption capacity expressed in mmol, b is the affinity constant, and n is the index of heterogeneity.

Isosteric heat of adsorption was calculated using the Clausius–Clapeyron equation (Equation (2)):

$$\ln \frac{P_2}{P_1} = -\frac{\Delta H}{R}\left(\frac{1}{T_2} - \frac{1}{T_1}\right) \tag{2}$$

where P_1 and P_2 refer to the relative pressure of the gas at T_1 and T_2, respectively, expressed in MPa; T_1 and T_2 refer to the temperature of 273 K (0 °C) and 295 K (25 °C), respectively; R is the ideal gas constant whose value is 8.314 J/(mol K); and ΔH is the enthalpy change of gas expressed in KJ/mol.

The adsorption selectivity of samples was calculated with the ideal adsorbed solution theory (IAST, Equation (3)):

$$S = \frac{x_1/x_2}{y_1/y_2} \quad (3)$$

where S refers to the adsorption selectivity of binary gas mixture; x_1 and x_2 are the molar fractions of adsorbed CO_2 and N_2 in the NBAC sample, respectively; and y_1 and y_2 are the molar fractions of CO_2 and N_2 in the binary gas phase, respectively.

4. Conclusions

In summary, in this work, an in situ dry chemical synthesis was employed to fabricate N-doped bamboo-based activated carbon (NBAC) from conventional bamboo charcoal applying sodamide as an activation material and nitrogen source with nitrogen protection at a medium temperature (400–600 °C) in this work. The as-synthesized NBAC with high nitrogen content and narrowly distributed micropores presented a specific surface area with 756–1489 m^2/g, excellent CO_2 adsorption performance, Among all the synthesized samples, NBACs obtained at 500 °C with a sodamide/bamboo charcoal blend ratio of 3:1, demonstrated the highest CO_2 adsorption of 4.95 mmol/g at 0 °C and 1 bar, fairly good CO_2/N_2 adsorption selectivity, low isosteric heat of adsorption, and good recycling and regeneration performance, which made the NBAC a candidate absorbent in CO_2 capture and utilization.

Author Contributions: Data curation, W.Y., S.T., H.L., Z.Z. and J.Z.; formal analysis, W.Y., S.T. and J.Z.; funding acquisition, W.Z.; investigation, W.Y., S.T., Z.Z., G.K., J.Z. and W.Z.; methodology, W.Z. and J.Z.; writing—review and editing, W.Y., W.Z. and J.Z. All authors have read and agreed to the published version of the manuscript.

Funding: This work was supported by the Science and Technology Key Project of Zhejiang, China (2021C03146).

Institutional Review Board Statement: Not applicable.

Informed Consent Statement: Not applicable.

Data Availability Statement: The data presented in this study are available on request from the corresponding authors.

Acknowledgments: The authors would like to thank the National Engineering and Technology Research Center of Wood-based Resources Comprehensive Utilization for providing the experimental platform in this work.

Conflicts of Interest: The authors declare that there is no commercial or associative interest that represent a conflict of interest in connection with the work submitted.

References

1. Sridhar, S.; Smitha, B.; Aminabhavi, T.M. Separation of carbon dioxide from natural gas mixtures through polymeric membranes—A Review. *Sep. Purif. Rev.* **2007**, *36*, 113–174. [CrossRef]
2. Xing, X.; Wang, R.; Bauer, N.; Ciais, P.; Cao, J.; Chen, J.; Tang, X.; Wang, L.; Yang, X.; Boucher, O.; et al. Spatially explicit analysis identifies significant potential for bioenergy with carbon capture and storage in China. *Nat. Commun.* **2021**, *12*, 3159. [CrossRef] [PubMed]
3. Rau, G.H.; Willauer, H.D.; Ren, Z. The global potential for converting renewable electricity to negative-CO_2-emissions hydrogen. *Nat. Clim. Chang.* **2018**, *8*, 621–625. [CrossRef]
4. Cai, Y.; Sam, C.Y.; Chang, T. Nexus between clean energy consumption, economic growth and CO_2 emissions. *J. Clean. Prod.* **2018**, *182*, 1001–1011. [CrossRef]
5. Zhuang, Y.; Simakov, D.S.A. Single-pass conversion of CO_2/CH_4 mixtures over the low-loading Ru/γ-Al_2O_3 for direct biogas upgrading intorenewable natural gas. *Energy Fuels* **2021**, *35*, 10062–10074. [CrossRef]
6. Siegelman, R.L.; Kim, E.J.; Long, J.R. Porous materials for carbon dioxide separations. *Nat. Mater.* **2021**, *20*, 1060–1072. [CrossRef] [PubMed]
7. Huang, K.; Chai, S.H.; Mayes, R.T.; Tan, S.; Jones, C.W.; Dai, S. Significantly increasing porosity of mesoporous carbon by $NaNH_2$ activation for enhanced CO_2 adsorption. *Microporous Mesoporous Mater.* **2016**, *230*, 100–108. [CrossRef]

8. Greig, C.; Uden, S. The value of CCUS in transitions to net-zero emissions. *Electr. J.* **2021**, *34*, 107004. [CrossRef]
9. Leflay, H.; Pandhal, J.; Brown, S. Direct measurements of CO_2 capture are essential to assess the technical and economic potential of algal-CCUS. *J. CO2 Util.* **2021**, *52*, 101657. [CrossRef]
10. Tcvetkov, P.; Cherepovitsyn, A.; Fedoseev, S. The changing role of CO_2 in the transition to a circular economy: Review of carbon sequestration projects. *Sustainability* **2019**, *11*, 5834. [CrossRef]
11. Li, D.; Zhou, J.; Wang, Y.; Tian, Y.; Wei, L.; Zhang, Z.; Qiao, Y.; Li, J. Effects of activation temperature on densities and volumetric CO_2 adsorption performance of alkali-activated carbons. *Fuel* **2019**, *238*, 232–239. [CrossRef]
12. Serafin, J.; Ouzzine, M.; Cruz, O.F., Jr.; Sreńscek-Nazzal, J.; Gómez, I.C.; Azar, F.Z.; Mafull, C.A.R.; Hotza, D.; Rambo, C.R. Conversion of fruit waste-derived biomass to highly microporous activated carbon for enhanced CO_2 capture. *Waste Manag.* **2021**, *136*, 273–282. [CrossRef]
13. Melouki, R.; Ouadah, A.; Llewellyn, P.L. The CO_2 adsorption behavior study on activated carbon synthesized from olive waste. *J. CO2 Util.* **2020**, *42*, 101292. [CrossRef]
14. Zgrzebnicki, M.; Kałamaga, A.; Wrobel, R. Sorption and textural properties of activated carbon derived from charred beech wood. *Molecules* **2021**, *26*, 7604. [CrossRef]
15. Kumar, R.; Zhang, C.; Itta, A.K.; Koros, W.J. Highly permeable carbon molecular sieve membranes for efficient CO_2/N_2 separation at ambient and subambient temperatures. *J. Membr. Sci.* **2019**, *583*, 9–15. [CrossRef]
16. Russo, F.; Galiano, F.; Iulianelli, A.; Basile, A.; Figoli, A. Biopolymers for sustainable membranes in CO_2 separation: A review. *Fuel Process. Technol.* **2021**, *213*, 106643. [CrossRef]
17. Granados-Correa, F.; Bonifacio-Martinez, J.; Hernandez-Mendoza, H.; Bulbulian, S. CO_2 capture on metallic oxide powders prepared through chemical combustion and calcination methods. *Water Air Soil Pollut.* **2015**, *226*, 281. [CrossRef]
18. Wang, S.; Wang, C.; Zhou, Q. Strong foam-like composites from highly mesoporous wood and metal-organic frameworks for efficient CO_2 capture. *ACS Appl. Mater. Interfaces* **2021**, *13*, 29949–29959. [CrossRef] [PubMed]
19. Gomez-Delgado, E.; Nunell, G.; Cukierman, A.L.; Bonelli, P. Tailoring activated carbons from pinus canariensis cones for post-combustion CO_2 capture. *Environ. Sci. Pollut. Res.* **2020**, *27*, 1–15. [CrossRef]
20. Khalil, S.H.; Aroua, M.K.; Daud, W.M.A.W. Study on the improvement of the capacity of amine-impregnated commercial activated carbon beds for CO_2 adsorbing. *Chem. Eng. J.* **2012**, *183*, 15–20. [CrossRef]
21. Yosefi, L.; Khoshbin, R.; Karimzadeh, R. Beneficial incorporation of metal-sulfur interaction in adsorption capacity of boron nitride based adsorbents used in highly selective sulfur removal. *Fuel* **2022**, *310*, 122277. [CrossRef]
22. Kwon, S.; You, Y.; Lim, H.; Lee, J.; Chang, T.-S.; Kim, Y.; Lee, H.; Kim, B.-S. Selective CO adsorption using sulfur-doped Ni supported by petroleum-based activated carbon. *J. Ind. Eng. Chem.* **2020**, *83*, 289–296. [CrossRef]
23. Ouzzine, M.; Serafin, J.; Sreńscek-Nazzal, J. Single step preparation of activated biocarbons derived from pomegranate peels and their CO_2 adsorption performance. *J. Anal. Appl. Pyrolysis.* **2021**, *160*, 105338. [CrossRef]
24. Pan, H.; Zhao, J.; Lin, Q.; Cao, J.; Liu, F.; Zheng, B. Preparation and characterization of activated carbons from bamboo sawdust and its application for CH_4 selectivity adsorption from a CH_4/N_2 system. *Energy Fuels* **2016**, *30*, 10730–10738. [CrossRef]
25. Idrees, M.; Rangari, V.; Jeelani, S. Sustainable packaging waste-derived activated carbon for carbon dioxide capture. *J. CO2 Util.* **2018**, *26*, 380–387. [CrossRef]
26. Huang, K.; Chai, S.-H.; Mayes, R.T.; Veith, G.M.; Browning, K.L.; Sakwa-Novak, M.A.; Potter, M.E.; Jones, C.W.; Wu, Y.-T.; Dai, S. An efficient low-temperature route to nitrogen-doping and activation of mesoporous carbons for CO_2 capture. *Chem. Commun.* **2015**, *51*, 17261–17264. [CrossRef] [PubMed]
27. Huang, K.; Li, Z.; Zhang, J.; Tao, D.; Liu, F.; Dai, S. Simultaneous activation and N-doping of hydrothermal carbons by NaNH2: An effective approach to CO_2 adsorbents. *J. CO2 Util.* **2019**, *33*, 405–412. [CrossRef]
28. Rao, L.; Liu, S.; Wang, L.; Ma, C.; Wu, J.; An, L.; Hu, X. N-doped porous carbons from low-temperature and single-step sodium amide activation of carbonized water chestnut shell with excellent CO2 capture performance. *Chem. Eng. J.* **2019**, *359*, 428–435. [CrossRef]
29. Bamdad, H.; Hawboldt, K.A.; MacQuarrie, S.L. Nitrogen functionalized biochar as a renewable adsorbent for efficient CO_2 removal. *Energy Fuels* **2018**, *32*, 11742–11748. [CrossRef]
30. Han, J.; Li Zhang, L.; Zhao, B.; Qin, L.; Wang, Y.; Xing, Y. The N-doped activated carbon derived from sugarcane bagasse for CO_2 adsorption. *Ind. Crops Prod.* **2018**, *128*, 290–297. [CrossRef]
31. Singh, G.; Kim, I.Y.; Lakhi, K.S.; Joseph, S.; Srivastava, P.; Naidu, R.; Vinu, A. Heteroatom functionalized activated porous biocarbons and their excellent performance for CO_2 capture at high pressure. *J. Mater. Chem. A* **2017**, *5*, 21196–21204. [CrossRef]
32. Rao, L.; Ma, R.; Liu, S.; Wang, L.; Wu, Z.; Yang, J.; Hu, X. Nitrogen enriched porous carbons from D-glucose with excellent CO_2 capture performance. *Chem. Eng. J.* **2019**, *362*, 794–801. [CrossRef]
33. Ren, Q.; Zeng, Z.; Xie, M.; Jiang, Z. Cement-based composite with humidity adsorption and formaldehyde removal functions as an indoor wall material. *Constr. Build. Mater.* **2020**, *247*, 118610. [CrossRef]
34. Yue, X.; Ma, N.L.; Sonne, C.; Guan, R.; Lam, S.S.; Van Le, Q.; Chen, X.; Yang, Y.; Gu, H.; Rinklebe, J.; et al. Mitigation of indoor air pollution: A review of recent advances in adsorption materials and catalytic oxidation. *J. Hazard. Mater.* **2021**, *405*, 124138. [CrossRef] [PubMed]
35. Balou, S.; Babak, S.E.; Priye, A. Synergistic effect of nitrogen doping and ultra-microporosity on the performance of biomass and microalgae-derived activated carbons for CO_2 capture. *ACS Appl. Mater. Interfaces* **2020**, *12*, 42711–42722. [CrossRef]

36. Zhao, Y.; Hao, R.; Qi, M. Integrative process of preoxidation and absorption for simultaneous removal of SO_2, NO and Hg^0. *Chem. Eng. J.* **2015**, *269*, 159–167. [CrossRef]
37. Tan, Z.; Sun, L.; Xiang, J.; Zeng, H.; Liu, Z.; Hu, S.; Qiu, J. Gas-phase elemental mercury removal by novel carbon-based sorbents. *Carbon* **2012**, *50*, 362–371. [CrossRef]
38. Peng, X.; Hu, F.; Zhang, T.; Qiu, F.; Dai, H. Amine-functionalized magnetic bamboo-based activated carbon adsorptive removal of ciprofloxacin and norfloxacin: A batch and fixed-bed column study. *Bioresour. Technol.* **2018**, *249*, 924–934. [CrossRef] [PubMed]
39. Huang, J.; Zimmerman, A.R.; Chen, H.; Gao, B. Ball milled biochar effectively removes sulfamethoxazole and sulfapyridine antibiotics from water and wastewater. *Environ. Pollut.* **2020**, *258*, 113809. [CrossRef]
40. Shi, R.; Li, J.; Ni, N.; Xu, R. Understanding the biochar's role in ameliorating soil acidity. *J. Integr. Agric.* **2019**, *18*, 1508–1517. [CrossRef]
41. Khuong, D.A.; Nguye, H.N.; Tsubota, T. Activated carbon produced from bamboo and solid residue by CO_2 activation utilized as CO_2 adsorbents. *Biomass Bioenergy* **2021**, *148*, 106039. [CrossRef]
42. Dilokekunakul, W.; Teerachawanwong, P.; Klomkliang, N.; Supasitmongkol, S.; Chaemchuen, S. Effects of nitrogen and oxygen functional groups and pore width of activated carbon on carbon dioxide capture: Temperature dependence. *Chem. Eng. J.* **2020**, *389*, 124413. [CrossRef]
43. Marsh, H.; Francisco Rodríguez-Reinoso, F. *Activated Carbon*; Elsevier Science Ltd.: Amsterdam, The Netherlands, 2006; pp. 322–365.
44. Sanchez-Sanchez, A.; Suarez-Garcia, F.; Martinez-Alonso, A.; Tascon, J.M.D. Influence of Porous Texture and Surface Chemistry on the CO_2 Adsorption Capacity of Porous Carbons: Acidic and Basic Site Interactions. *ACS Appl. Mater. Interfaces* **2014**, *6*, 21237–21247. [CrossRef] [PubMed]
45. Chen, J.; Yang, J.; Hu, G.; Hu, X.; Li, Z.; Shen, S.; Radosz, M.; Fan, M. Enhanced CO_2 capture capacity of nitrogen-doped biomass-derived porous carbons. *ACS Sustain. Chem. Eng.* **2016**, *4*, 1439–1445. [CrossRef]